followed by CH_2Cl_2 afforded unreacted α,α'-dibromo-p-xylene. Elution with a mixture of *n*-hexane and ethyl acetate(2:1, v/v, 85 m*l*) gave an unknown compound(11 mg). Elution with the same solvent mixture(1:1, v/v, 60 m*l*) gave **23**(112 mg, 0.15 mmoles, 2%); ^{1}H NMR($CDCl_3$) δ 4.45(s, 4H), 4.64(s, 4H), 5.26(s, 4H, $2NCH_2$), 7.00-7.50(m, 18H, ArH), 7.66-7.94(m, 2H, ); MS *m/e*(Rel. int) 183(58.1, 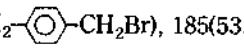), 185(53.5, 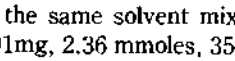). Elution with the same solvent mixture (1:2, v/v, 100 m*l*) gave **24** (1,191mg, 2.36 mmoles, 35%): ^{1}H NMR($CDCl_3$ + DMSO-d_6, 5:1, v/v) δ 4.50(s, 4H, $2SCH_2$), 5.23(s, 4H, $2NCH_2$), 6.61 (s, 4H, 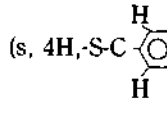), 6.94(s, 4H, 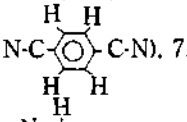), 7.13-7.44 (m, 6H, ArH), 7.58-7.90 (m, 2H, 2 ); MS *m/e* 540 (M^+).

Reaction of 22 with 2. Sodium naphthalenide (**2**) was added to a suspension of **22** (1,433 mg, 3.56 mmoles) in 30 m*l* of THF at room temperature under N_2 atmosphere until green color of **2** persisted. The reaction mixture was quenched with water, followed by the extraction with ethyl acetate. After the solvent was evaporated, the residue was chromatographed. Elution with chloroform(130 m*l*) afforded a mixture of naphthalene and 1,2-di-p-tolylethane[11] (228 mg, 1.08 mmoles, 61%). Elution with acetone(80 m*l*) gave **1**(869 mg, 5.79 mmoles, 81%).

Reaction of 24 with 2. As in the reaction of **22**, **2** was added to a suspension of **24**(965 mg, 1.91 mmoles) in 30 m*l* of THF. The reaction mixture was worked up as in the previous reaction. Elution with *n*-hexane(150 m*l*) gave a mixture of naphthalene and 1,2-di-p-tolyethane. Elution with a mixture(90 m*l*) of *n*-hexane and ethyl acetate(3:1, v/v) gave 1-(*p*-tolylmethyl) benzimidazoline-2-thione(**25**, 155 mg, 0.61 mmoles, 32%): mp 201-202 °C (ethyl acetate-n-hexane, 1:10, v/v); ^{1}H NMR($CDCl_3$-DMSO-d_6, 3:1, v/v) δ 2.24(s, 3H, Me), 5.49(s, 2H, CH_2), 6.88-7.34(m, 8H, ArH), 12.60(s, 1H, NH); MS *m/e* 254(M^+). Elution next with the same solvent mixture(2:1, v/v, 170 m*l*) gave an unknown (157 mg) and **1**(282 mg, 1.88 mmoles, 49%).

Acknowledgement. Support of this work by Korea Science and Engineering Foundation is gratefully acknowledged.

References

1. (a) J. A. Vida, *Tetrahedron Letts.*, 3921 (1972).
(b) C. Rovnyah, V. L. Narayana, R. D. Haugwitz, and C. M. Cimarusti, U.S. Patent 3,927,014 (1975); *Chem. Abstr.*,**84** , 105596m (1976).
2. (a) R. J. Badger and G. B. Barlin, *J. Chem. Soc.* Perkin II. 1176 (1976).
(b) E. Hoggarth, *J. Chem. Soc.*, 3311 (1949).
3. O. P. Suri, R. K. Khajuria, D. B. Saxena, N. S. Rawat, and C. K. Atal, *J. Heterocyclic Chem.*,**20,** 813 (1983).
4. (a) B. Stanovnik, M. Tisler, A. Hribar, G. B. Barlin, and D. J. Brown, *Aust. J. Chem.*,**34,** 1729 (1981).
(b) E. V. Logachev, M. V. Povstanyanoi, P. M. Kochergin, Yu.I. Beilis, *Izv. Vyssh. Uchebn.* Zaved. *Khim. Khim. Tekhnol.* **19,** 1039 (1976); *Chem. Abstr.*, **85,** 159984a (1977).
(c) N. P. Bednyagina and I. Ya. Postovskii, Nauch. Doklady Vysshei, Shkoly, Khim. Khim. Tekhnol, No. 2, 333 (1959); *Chem. Abstr.*,**54,** 510b (1960).
(d) K. V. Ananeva, N. K. Rozhkova, *Uzb. Khim. Zh.* **17,** 56 (1973); *Chem. Abstr.*, **62**, 13140f(1965).
5. A manuscript has been submitted to *J. Heterocyclic Chem.*
6. N. L. Holy, *Chem. Rev.*, **74**(2), 243 (1974); References are cited therein.
7. J. F. Bunnett, *Accounts Chem. Res.*, **11,** 413 (1978).
8. (a) S. Bank and B. Bockrath, *J. Am. Chem. Soc.*, **93,** 430 (1971).
(b) J. F. Garst, *Accounts Chem. Res.*, **4**, 400 (1971).
9. K. Futaki, *J. Pharm. Soc. Jap.*,**74,** 1365 (1954).
10. G. N. Tyurenkova, E. I. Silina, and I. Ya. Postovskii, *Zhur. Priklad. Khim.* **34,** 2327 (1961); *Chem. Abstr.*, **56,** 7303d (1962).
11. S. Kunichika, S. Oka, and T. Sugiyama, *Bull. Inst. Chem. Res., Kyoto Univ.* **43**(3), 250(1965); *Chem. Abstr.*, **64,** 4972c (1966).

Topological Approach to the Rubber Elasticity of Polymer Networks

Jung Mo Son and Hyungsuk Pak*

Department of Chemistry, Seoul National University, Seoul 151-742. *Received October 4, 1988*

Applying the topological theory of rubber elasticity which was suggested by K. Iwata to the newly devised body-centered cubic lattice model, the authors calculated the values of four terms of the free energy to form polymer networks. Finding the projection matrix of the BCL model, and comparing this with the values of the simple cubic lattice (abbreviated to SCL hereafter) model of K. Iwata, the authors obtained the stress versus strain curves and found that the curves are in good agreement with the experimental results of poly(dimethyl siloxane) networks.

Introduction

Rubber elasticity theories are classified into two categories. One is the phantom network theories (PNT)[1-12] and the other the topological ones (TNT)[13-15]. In the former, the stress of networks is regarded as coming from the entropic

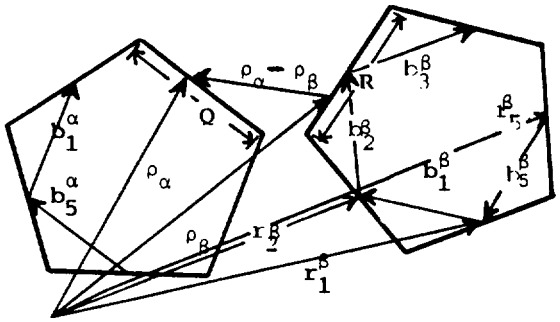

Figure 1. A diagram representing GLC's and position vectors ρ's and bond vectors b's in two loops α and β. Q and R denotes momentary variation fields of S_α and S_β, respectively. ρ_k is a parameteric position vector determined by a parameter S_k which takes the variation field within the segment at any moment, the subscript k being α or β for loops.

forces acting between ends of cross-linked polymers (strands), while in the latter, it is regarded as coming from the topological forces among entwing strands. It is believed that both the entropic forces and the topological ones contribute to rubber elasticity. But it is yet in controversy which is the main factor of this phenomenon. To solve the problem, the two forces must be considered simultaneously on the same theoretical background. This approach has first been tried by Deam and Edwards.[13]

In the present work, the authors propose a newly devised model of which the junction points form a body-centered cubic lattice and four strands connected to a junction point make a tetrahedral arrangement (hereafter, we call it the BCL model). Applying the topological rubber elasticity theory of K. Iwata[16-18] to this BCL model of networks, the authors calculated the projection matrix $\Gamma^{\#}$ which is the most important factor necessary to calculate the free energy of networks, and obtained the stress versus strain curve of poly (dimethyl siloxane).

Transformation Matrices

The important idea[17] of a topological theory is that of the interaction among strands in the network. A word *strand* means a polymer chain which joins two neighboring junction points. A word *junction point* means the jointing part of strands in the networks.

In the TNT or PNT, polymers having elasticity are regarded as composed of the network which consists of a great number of junction points and strands. In general lattice models, a fundamental unit, which describes the physical properties of the whole network system, is called a cell.

In the TNT, it is assumed that the network, is a set of regular arrangement of cells. Three assumptions of the TNT are as follows:

(1) The network is composed of N_c identical cells, each of which consists of sufficiently large number of strands and junction points. Let N_T be the number of total junction points of the network.

(2) The network is a set of cyclic arrangement of cells.

(3) Under a strain relative displacements of mass centers of cells are exactly affinelike.

It is necessary to introduce the conception of a GLC

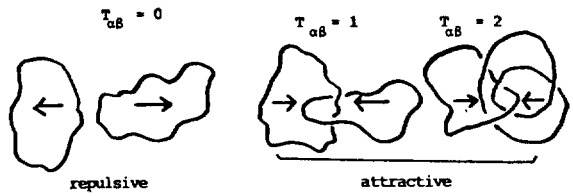

Figure 2. Topological states and GLC's, *i.e.*, $T_{\alpha\beta}$'s, for the ring polymers α and β. If $T_{\alpha\beta} = 0$, then there is a repulsive force between loops, otherwise there is an attractive force.

(Gauss Linking Coefficient). Let's define $T_{\alpha\beta}$ to be the GLC between loops α and β and θ_{ab} the GLC between strands a and b as follows:

$$T_{\alpha\beta}=\frac{1}{4\pi}\oint_\alpha\oint_\beta\frac{(\dot\rho_\alpha\times\dot\rho_\beta)\cdot(\rho_\alpha-\rho_\beta)}{|\rho_\alpha-\rho_\beta|^3}dS_\alpha dS_\beta \tag{1}$$

$$\theta_{ab}=\int_{r_a}^{r_a'}\int_{r_b}^{r_b'}\frac{(\dot\rho_a\times\dot\rho_b)\cdot(\rho_a-\rho_b)}{|\rho_a-\rho_b|^3}dS_a dS_b \tag{2}$$

where ρ_k is a position vector determined by a parameter S_k which takes the variation field within the segment at any moment and $\dot\rho_k = d\rho_k/dS_k$, the subscript k being α or β for loops and a or b for strands. The picture illustrating the meanings of Eqs. 1 and 2 is given in Figure 1. Here two pentagonal loops α and β are shown. Loops α and β are composed of five segments respectively. Position vectors of segments in loops are represented as the ones joined directly from the origin of the network system to center points of segments. If we let r^α and r^β be the sets of position vectors of loops α and β, respectively, we have

$$\begin{aligned} r^\alpha &= \{r_1^\alpha, r_2^\alpha, r_3^\alpha, r_4^\alpha, r_5^\alpha\} \\ r^\beta &= \{r_1^\beta, r_2^\beta, r_3^\beta, r_4^\beta, r_5^\beta\}. \end{aligned} \tag{3}$$

A bond vector b, which joins the center points of two neighboring segment, is defined by

$$b_{i+1} - r_i. \tag{4}$$

The sets of bond vectors b^α and b^β of loops and β are given by

$$\begin{aligned} b^\alpha &= \{b_1^\alpha, b_2^\alpha, b_3^\alpha, b_4^\alpha, b_5^\alpha\} \\ b^\beta &= \{b_1^\beta, b_2^\beta, b_3^\beta, b_4^\beta, b_5^\beta\}. \end{aligned} \tag{5}$$

In general, there are a great number of loop GLC's, such as T_i, T_j, and etc. Let T_0 and θ be the sets of loop and strand GLC's, respectively. Let T_1 be a subset which meets the condition that all elements of T_0 should be represented as linear combinations of elements of T_1. Now the transformation matrices between the sets of loop and strand GLC's are given by

$$\begin{aligned} T_0 &= \theta C \\ T_1 &= T_0 B \\ T_1 &= \theta \Gamma \\ \Gamma &= CB \end{aligned} \tag{6}$$

where T_0, T_1, and θ are n_0, n_1, and n_2 dimensional row vectors, respectively, and Γ is $n_2 \times n_1$ dimensional matrix. n_0 is the number of GLC's of T_0, n_1 that of GLC's of T_1, and n_2 that of GLC's of θ. Let τ be any element of T_1, r^0 the set of position vectors of junction points in the reference state, and r the set of those in any state. For a given state let F be the free energy of the system, Ψ the topological distribution

function, and $V(\lambda)$ the volume under the macroscopic strain λ, then the free enrgy $F(\lambda,r^0)$[17] is given by

$$F(\lambda, r^\circ) = \sum_\tau \{-kT\ln \int_{r\in\lambda} \Psi(r, \tau)\, dr\}\, \Psi(\tau|r^\circ) \quad (7)$$

where $\Psi(\tau|r^0)$ is the conditional distribution function given as a function of τ when the position vectors are fixed at r^0. The total free energy of the network F may be separated into four terms as follows:

$$F = F_{0,ph} + F_{0,top} + F_1 + F_2 \quad (8)$$

where $F_{0,ph}$ is a term coming from the entropic force acting between ends of the strands, and $F_{0,top}$ is one coming from the topological interaction among the strands when all the junction points deform affinely. F_1 is a correction term due to nonaffine displacement of the junction points, and F_2 is one due to the fluctuation of θ. Transition matrices of Eq. 6 contribute only to F_2.

It is likely good to go on after considering the meanings of $T_{\alpha\beta}$. As shown in Figure 2, $T_{\alpha\beta}$ has the only integer values. When $T_{\alpha\beta} = 0$ there is a repulsive force, while in case that $T_{\alpha\beta} \neq 0$ there is an attractive force between loops α and β.

A generalized inverse[26] of any matrix A is defined by

$$A^+ \equiv (A^tA)^{-1}A^t \quad (9)$$

where A^t, of course, is a transpose of A, and $(A^tA)^{-1}$ is an inverse matrix of A^tA. The projection matrices of Γ and C are given by, respectively,

$$\Gamma^\# \equiv \Gamma(\Gamma^t\Gamma)^+\Gamma^t$$
$$C^\# \equiv C(C^tC)^+C^t. \quad (10)$$

According to proofs[17] of matrix relationships,

$$\Gamma^\# = C^\#$$
$$Tr\,\Gamma^\# = Tr\,C^\# = n_1 \quad (11)$$

whre n_1 is the number of elements of T_1. In other words, n_1 is the number of effective loop pairs. $\Gamma^\#$ should be found according to the given model of the network as shown later more clearly.

Distribution Function and Free Energy

In the PNT or TNT, the free energy of networks is obtained from the distribution functions of junction points and strands. The conditional distribution function $\Psi(\tau|r)$ is given by

$$\Psi(\tau|r) = \int_{\tau-1/2}^{\tau+1/2} \int \delta(t-\theta\Gamma) \prod_p \{(1-G_p/H_p)\delta(\theta_p) + (G_p/H_p)2\pi H_p)^{-1/2} \cdot \exp(-\theta_p^2/2H_p)\}\, d\theta\ dt \quad (12)$$

where δ is a delta function. G_P and H_P are given by, respectively

$$G_p(r) = \nu'^2 \gamma g_p(r) \quad (13)$$
$$H_p(r) = \nu'^2 \gamma h_p(r) \quad (14)$$

where γ is a characteristic parameter for the given model, and ν' is the number of submolecules included in a strand. It is assumed that every strand has the same number of submolecules, and that every submolecules has the same number of segments. In Eqs. 13 and 14, p stands for the bond pair of the strands a and b, and r is represented by

$$r = \{r_a, r'_a, r_b, r'_b\} \quad (15)$$

where r_a and r'_a are the position vectors of end points of the strand a, and r_b and r'_b are those of the strand b. Let the letter μ denote the bond pair of the submolecules a_i and b_j and the letter μ' that of the submolecules a'_i and b'_j. When the vector r is fixed, let $P_{ph}(O_\mu|r)$ be the distribution function of single contact obtained when the bond pair μ is formed, and $P_{ph}(O_{\mu,\mu'}|r)$ that of double contact obtained when the bond pairs μ and μ' are formed between two strands in a phantom network. Then the $g_p(r)$ and $h_p(r)$ in Eqs. 13 and 14 are given by

$$g_p(r) = \nu'^{-2} \sum_{\mu=1}^{\nu'^2} P_{ph}(O_\mu|r) \quad (16)$$
$$h_p(r) = \nu'^{-2}[g_p(r)]^{-1} \sum_{\mu=1}^{\nu'^2} \sum_{\mu'=1}^{\nu'^2} P_{ph}(O_{\mu,\mu'}|r)$$

where $g_p(r)$ is the value of the mean single contact probability and $h_p(r)$ that of the mean double contact one between submolecules in two strands.

The distribution functions $\Psi(r,\tau)$ and $\Psi(\tau|r^0)$ can be expressed as

$$\Psi(r, \tau) = P_{ph}(r)\, \Psi(\tau|r) \quad (17)$$
$$\Psi(\tau|r^\circ) = \int_{\tau-1/2}^{\tau+1/2} \Psi_1(t|r^\circ)\, dt$$

where $P_{ph}(r)$ is the distribution function of junction points in a phantom network. When the network is in the topological state τ and occupies a volume $V(\lambda)$ whose shape is determined by λ, its free energy is defined by

$$F(\lambda, \tau) = -kT \ln \int_{r\in\lambda} \Psi(r, \tau)\, dr. \quad (18)$$

Then the free energy averaged over the set of r^0 is given by

$$F(\lambda, r^\circ) = \sum_\tau F(\lambda, \tau)\, \Psi(\tau|r^\circ). \quad (19)$$

Detailed Form of the Free Energy

The derivative of the total free energy of the network F with respect to λ can be given as follows[17]:

$$\frac{\partial F}{\partial \lambda} = \frac{\partial F_{0,ph}}{\partial \lambda} + \frac{\partial F_{0,top}}{\partial \lambda} + \frac{\partial F_1}{\partial \lambda} + \frac{\partial F_2}{\partial \lambda} \quad (20)$$

$$\frac{\partial F_{0,ph}}{\partial \lambda} = 3\sum_s \frac{1}{l_s^2}(\dot{r}_s^{*\prime} - \dot{r}_s^*) \quad (21)$$

$$\frac{\partial F_{0,top}}{\partial \lambda} = -kT\sum_p \{(\frac{\dot{g}_p^*}{g_p^*} - \frac{\dot{h}_p^*}{h_p^*})(\frac{g_p^\circ}{h_p^\circ} - \frac{g_p^*(g_p^\circ - h_p^\circ)}{h_p^\circ(g_p^* - h_p^*)}) + \frac{\dot{h}_p^*}{2h_p^*} \cdot (\frac{g_p^\circ}{h_p^*} - \frac{g_p^\circ}{g_p^*})\} \quad (22)$$

$$\frac{\partial F_1}{\partial \lambda} = -\frac{kT}{2} Tr[<W^*>(<W^*>)^+ - 2<\dot{V}^*V^*>(<W^*>)^+ + <V^*V^*>(<W^*>)^+ <\dot{W}^*> \cdot (<W^*>)^+] \quad (23)$$

$$\frac{\partial F_2}{\partial \lambda} = -\frac{kT}{2}[\sum_p (\bar{\Gamma}_{pp}^\#)^2 \frac{\dot{h}_p^*}{h_p^*}(\frac{g_p^\circ}{h_p^\circ} - \frac{g_p^\circ}{h_p^*}) + \sum_p \sum_{p'} (\bar{\Gamma}_{pp'}^\#)^2 \frac{g_p^\circ h_{p'}^{\circ *}}{(h_p^*)^3} \cdot \frac{g_{p'}^\circ \dot{h}_{p'}^*}{h_{p'}^{\circ *}}]. \quad (24)$$

The above Eqs. 20 to 24 are main parts of the TNT. Now it is likely good to consider the physical meanings of all terms in Eqs. 20 to 24. The letter s of Eq. 21 stands for any strand in the network, and l_s^2 is the mean squared end-to-end distance of the strand s in the phantom network. The position vectors of end points in the strand s are expressed as r_s' and r_s. The symbol dot (.) denotes the first derivatives of given functions in regard to λ, such as

$$\dot{r}_s^{*\prime} = \frac{\partial r_s^{*\prime}}{\partial \lambda}, \quad \dot{r}_s^{*} = \frac{\partial r_s^{*}}{\partial \lambda}, \quad \dot{g}_p^{*} = \frac{\partial g_p^{*}}{\partial \lambda}, \quad \cdots\cdots \tag{25}$$

In the above equations, the superscript o attached on the g_p and h_p represents that they are the values at $r = r^0$ and the superscript * attached on the g_p, h_p, V, W, and etc. denotes that they are the ones at $r = r^*$, r^* being the set of position vectors of junction points deformed affinelikely under the macroscopic strain λ. Also the g_p and h_p, of course, are given by Eq. 16. Note that the usage of the superscripts o's and *'s just defined will be fixed throughout this paper.

Now a new function U is defined by

$$U = -\ln \phi(\theta, r)\,|_{\theta=\theta^0} \tag{26}$$

where $\phi(\theta, r)$ is the distribution function expressed as variables of θ and r. Letting M_0 be the number of junction points in a cell, which is the fundamental unit of lattices, the new quantities V^* and W^* are defined by

$$V_i^* = \frac{\partial}{\partial r_i} U|_{r=r^*} \tag{27}$$

$$W_{ij}^* = \frac{\partial}{\partial r_i}\frac{\partial}{\partial r_j} U|_{r=r^*} \tag{28}$$

where V^* is an M_0 dimensional super vector whose ith element is V_i^*, and W^* is an $M_0 \times M_0$ super matrix whose i,j element is W_{ij}^*. Recall that in a network n_1 is the number of effective loop pairs and that n_2 is the one of effective strand pairs. $\Gamma^{\#}$, which is an $n_2 \times n_2$ dimensional matrix, of Eq. 24 is

$$\Gamma^{\#} = \mathbf{1} - \Gamma^{*} \tag{29}$$

where $\Gamma^{\#}$ has been given in Eq. 10, and $\mathbf{1}$ is an $n_2 \times n_2$ unit matrix.

To find the free energy of a network, we have only to calculate terms of the right-hand side of Eqs. 22 to 24. The detailed method[16,17] to calculate the values of the g_p, h_p and etc. of Eq. 22 will be discussed in Section 5, and the detailed process to calculate the values of the $<V^*>$, $<V^*V^*>$, $<W^*>$, and etc. of Eq. 23 will be stated in Section 6. By using the newly devised BCL model, the detailed method of calculation of $\Gamma^{\#}$ of Eq. 24 will be shown in Sections 7 and 8.

g_p and h_p, and Their Derivatives

Recall that the relationships and physical meanings of the $g_p(r)$, $h_p(r)$, $P_{ph}(O_u|r)$, and $P_{ph}(O_u, O_u|r)$ have already been shown in Section 3. To calculate the $g_{ab}(r)$ and $h_{ab}(r)$, it is necessary to know two contact probabilities, the $P_{ph}(O_{aubv})$ and $P_{ph}(O_{aubv}, O_{au'bv'}|r)$ for the submolecular pairs (au,bv) and (au',bv') when the terminal points of strands a and b are fixed at $r = (r_a, r_a', r_b, r_b')$. In the absence of the excluded volume effect among the submolecules, the former is given by

$$P_{ph}(O_{aubv}|r) = (3\nu'^2/2\pi l^2 u\bar{u}v\bar{v}k_1)^{3/2} \cdot \exp[-3(k_3 - k_2^2/k_1)/2l^2] \tag{30}$$

where the k_1, k_2, and k_3 are expressed by

$$\begin{aligned} k_1 &= \nu'/u\bar{u} + \nu'/v\bar{v} \\ k_2 &= r_a/u + r_a'/\bar{u} + r_b/v + r_b'/\bar{v} \\ k_3 &= r_a^2/u + r_a'^2/\bar{u} + r_a^2/v + r_a'^2/\bar{v} - (r_a - r_a')^2/\nu' \\ &\quad - (r_b - r_b')^2/\nu'. \end{aligned} \tag{31}$$

The latter having two cases according to conditions is represented by

$$\begin{aligned} &P_{ph}(O_{aubv}, O_{au\ bv}|r) = \\ &(9\nu'^2/4\pi^4 l^4 u\bar{u}v\bar{v}u'v'\Delta u\Delta v \ \|K_1\|)^{3/2} \cdot \\ &\exp[-3(K_3 - K_2K_1^{-1}K_2)/2l^2] \end{aligned} \tag{32}$$

where one of the two cases included in Eq. 32 above has the conditions that $u>u'$ and $v>v'$ and that the K_1, K_2, and K_3 are given by

$$\begin{aligned} K_1 &= \begin{pmatrix} 1/\bar{u}+1/\bar{v}+1/\Delta u+1/\Delta v & -1/\Delta u-1/\Delta v \\ -1/\Delta u-1/\Delta v & 1/u'+1/v'+1/\Delta u+1/\Delta v \end{pmatrix} \\ K_2 &= \begin{pmatrix} r_a'/\bar{u}+r_b'/\bar{v} \\ r_a/u'+r_b/v' \end{pmatrix} \\ K_3 &= r_a'^2/\bar{u}+r_a^2/u'+r_b'^2/\bar{v}+r_b^2/v' \\ &\quad -(r_a-r_b')^2/\nu'+(r_b-r_b')^2/\nu' \end{aligned} \tag{33}$$

and the other has the conditions that $u>u'$ and $v<v'$ and that the K_1, K_2, and K_3 are given by

$$\begin{aligned} K_1 &= \begin{pmatrix} 1/\bar{u}+1/v'+1/\Delta u+1/\Delta v & -1/\Delta u-1/\Delta v \\ -1/\Delta u-1/\Delta v & 1/u'+1/\bar{v}+1/\Delta u+1/\Delta v \end{pmatrix} \\ K_2 &= \begin{pmatrix} r_a'/\bar{u}+r_b/v' \\ r_a/u'+r_b'/\bar{v} \end{pmatrix} \\ K_3 &= r_a'^2/\bar{u}+r_a^2/u'+r_b'^2/\bar{v}+r_b^2/v' \\ &\quad -(r_a-r_a')^2/\nu'+(r_b-r_b')^2/\nu' \end{aligned} \tag{34}$$

where ν' is the number of submolecules in the strands, the u,u',v, and v' are abbreviations of the au,au',bv, and bv', l^2 is the root mean squared end-to-end length of the submolecule, and $\bar{u} = \nu'-u$, $\bar{v} = \nu'-v$, $\Delta u = |u-u'|$, and $\Delta v = |v-v'|$.

Considering Eq. 30, we know that the $P_{ph}(O_{aubv}|r)$ has the form of the typical distribution function between submolecules in the strands a and b in a phantom network. Application twice of Eq. 30 leads to the formulation of $P_{ph}(O_{aubv}, O_{au'bv'}|r)$. For this the forms of $P_{ph}(O_{aubv}, O_{au'bv'}|r)$ are separated into two cases according to the relative positions of submolecules in strands and to the states of the distribution between strands. Both of them have, like the $P_{ph}(O_{aubv}|r)$, the forms of the typical distribution function of a phantom network. By use of Eqs. 30 and 32, the g_{ab} and h_{ab} can be calculated.

The reduced distance d, which is a linear length joining straight two centers of strands a and b, is expressed by

$$d = \frac{|r_a + r_a' - r_b - r_b'|}{2\sqrt{\nu}\, b} \tag{35}$$

where b in the denominator of the right-hand side denotes the

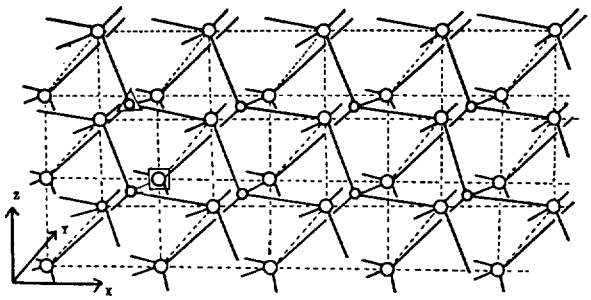

Figure 3. A diagram representing the tetrahedral structure of the BCL model whose junction points are composed of body-centered cubic lattices. Small circles represent the junction points, straight lines the strands, and dotted lines the edges of lattices.

length of a segment, and ν the degree of polymerization of a strand, that is, the number of segments of which a strand consists.

From Eqs. 16, 30, and 32, we know that the $g_{ab}(r)$ and $h_{ab}(r)$ can be expressed as functions of d, such as the $g_{ab}(d)$ and $h_{ab}(d)$. Derivatives of the $g_{ab}(r)$, $h_{ab}(r)$, and etc. in regard to r are calculated by

$$\frac{\partial g_{ab}(r)}{\partial r_a} = \frac{\partial g_{ab}(r)}{\partial d} \cdot \frac{\partial d(r_a, r'_a, r_b, r'_b)}{\partial r_a}$$
$$\cdots\cdots\cdots$$
$$\frac{\partial h_{ab}(r)}{\partial r'_b} = \frac{\partial h_{ab}(d)}{\partial d} \cdot \frac{\partial d(r_a, r'_a, r_b, r'_b)}{\partial r'_b} \tag{36}$$

$<V^*>$, $<V^*V^*>$, $<W^*>$, and Their Derivatives

We see that the explanation of V and W has already been given in Section 4. The averages of the V^*, V^*V^*, and W^* are all the functions of r^*, r^* (whose definition is given in Section 4) being expressed by

$$r^* = r^r \Lambda \tag{37}$$

where r^r is the position vector of junction points in the reference state, and Λ the diagonal matrix formed by three components of a macroscopic strain λ as follows:

$$\Lambda = \begin{pmatrix} \lambda_1 & & \\ & \lambda_2 & \\ & & \lambda_3 \end{pmatrix} \tag{38}$$

From the cyclic nature of cells, the $<V^*>$, $<V^*V^*>$, and $<W^*>$ can be described by the character of strands and junction points in a cell. Their components are expressed by

$$<V_i^*> = V_{ph,i}^* + \sum_\rho <V_{\rho,i}^*> \tag{39}$$

$$<V_i^* V_i^*> = <V_i^*><V_i^*> + \sum_\rho [<V_{\rho,i}^* V_{\rho,i}^*> - <V_{\rho,i}^*><V_{\rho,i}^*>] \tag{40}$$

$$<W_{ii}^*> = W_{ph,ii}^* + \sum_\rho <W_{\rho,ii}^*> \tag{41}$$

where the $V_{ph,i}^*$ and $W_{ph,ii}^*$ are components of the V^* and W^* in a phantom network, respectively. The $V_{ph,i}^*$ and $W_{ph,ii}^*$ are given by

$$V_{ph,i}^* = -\frac{3}{\nu' l^2} \sum_{i' \in n_i} (r_{i'}^* - r_i^*) \tag{42}$$

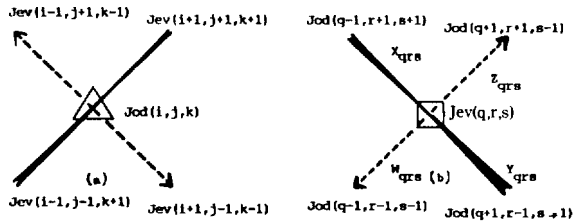

Figure 4. The definition of orientation of strands and general bond modes around J_{od}'s(a) and J_{ev}'s(b).

$$W_{ph,ii}^* = \begin{cases} -(3/\nu' l^2) N_i & \text{for } l' = l \\ (3/\nu' l^2) & \text{for } l' \in n_i \\ 0 & \text{otherwise} \end{cases} \tag{43}$$

where ν' is the number of submolecules in a strand, and l^2 is the mean squared end-to-end distance of a submolecule. n_i is the set of all the neighboring junction points with which a strand combines, and N_i the number of elements of n_i. For example, N_i has the value of 6 for the SCL model, and 4 for the BCL.

$<V_{\rho,i}^*>$, $<V_{\rho,i}^* V_{\rho,r}^*>$, and $<W_{\rho,ii}^*>$ in Eqs. 39 to 41 are given by

$$<V_{\rho,i}^*> = A_{\rho,i}^*(1 - g_\rho^\circ/h_\rho^\circ) + B_{\rho,i}^*(g_\rho^\circ/h_\rho^\circ) + C_{\rho,i}^* g_\rho^\circ \tag{44}$$

$$<V_{\rho,i}^* V_{\rho,r}^*> = A_{\rho,i}^* A_{\rho,r}^*(1 - g_\rho^\circ/h_\rho^\circ) + B_{\rho,i}^* B_{\rho,r}^*(g_\rho^\circ/h_\rho^\circ) + (B_{\rho,i}^* C_{\rho,r}^* + C_{\rho,i}^* B_{\rho,r}^*) g_\rho^\circ + C_{\rho,i}^* C_{\rho,r}^* g_\rho^\circ h_\rho^\circ \tag{45}$$

$$<W_{\rho,ii}^*> = A_{\rho,ii}^*(1 - g_\rho^\circ/h_\rho^\circ) + B_{\rho,ii}^*(g_\rho^\circ/h_\rho^\circ) + C_{\rho,ii}^* g_\rho^\circ \tag{46}$$

where the g_ρ^0 and h_ρ^0 are the values of the g_ρ and h_ρ, respectively when $r = r^0$. Terms appearing in the right-hand side of the above equations take the form of

$$A_{\rho,i}^* = (g_{\rho,i}^* - h_{\rho,i}^*) g_\rho^* / (g_\rho^* - h_\rho^*)$$
$$B_{\rho,i}^* = g_{\rho,i}^* - 3h_{\rho,i}^*/2$$
$$C_{\rho,i}^* = h_{\rho,i}^*/2h_\rho^*$$
$$A_{\rho,ii}^* = (g_{\rho,ii}^* - h_{\rho,ii}^* - g_{\rho,i}^* g_{\rho,r}^* + h_{\rho,i}^* h_{\rho,r}^*) g_\rho^* / (g_\rho^* - h_\rho^*) - (g_{\rho,i}^* - h_{\rho,i}^*)(g_{\rho,r}^* - h_{\rho,r}^*) g_\rho^* h_\rho^* / (g_\rho^* - h_\rho^*)^2$$
$$B_{\rho,ii}^* = g_{\rho,ii}^* - 3h_{\rho,ii}^*/2 - g_{\rho,i}^* g_{\rho,r}^* - 3h_{\rho,i}^* h_{\rho,r}^*/2 \tag{47}$$
$$C_{\rho,ii}^* = (h_{\rho,ii}^* - 2h_{\rho,i}^* h_{\rho,r}^*)/2h_\rho^* g_{\rho,r}^* h_{\rho,r}^* g_{\rho,ii}^*$$

where the $g_{\rho,i}^*$, $h_{\rho,i}^*$, $g_{\rho,ii}^*$, and $h_{\rho,ii}^*$ are given by

$$g_{\rho,i}^* = (\partial/\partial r_i^*) \ln g_\rho^*$$
$$h_{\rho,i}^* = (\partial/\partial r_i^*) \ln h_\rho^*$$
$$g_{\rho,ii}^* = (\partial/\partial r_i^*)(\partial/\partial r_i^*) \ln g_\rho^* \tag{48}$$
$$h_{\rho,ii}^* = (\partial/\partial r_i^*)(\partial/\partial r_i^*) \ln h_\rho^*.$$

Calculations of the $<\dot{V}_i^* \dot{V}_{i'}^*> + <V_i^* \dot{V}_{i'}^*>$ and $<\dot{W}_{ii}^*>$ are carried out by differentiating the $<V_i^* V_{i'}^*>$ and $<W_{ii}^*>$ in regard to λ, respectively. By using Eqs. 23, 39, 40, and 41, we can calculate F_1. By use of Eqs. 16, 30, and 32, we can obtain the value of $F_{0,top}$ from Eq. 22. By reading coordinates of position vectors of junction points, we can compute $F_{0,ph}$ readily from Eq. 21. Now it is the calculation of F_2 from Eq. 24 to be left to us. For this work we should find $\Gamma^{\#}$, which is

determined specifically according to any model given.

Thus, we will suggest the new model, that is, the BCL model, which is the first created by the authors, in Section 7, and originally give a series of equations due to the model. Furthermore in Section 8, we will show the detailed process for the calculation of the projection matrices of the new model.

BCL Model

The picture of the three dimensional structure of the BCL model is given in Figure 3, where solid lines denote strands and small circles represent junction points. Considering only the arrangement of junction points, we see that the three dimensional structure is a collection of typical body-centered cubic lattices. But the arrangement of strands around any junction point takes the form of a typical tetrahedral structure.

In the BCL model, junction points are classified into two categories according to the methods of their combination with neighboring strands. One is the set of junction points corresponding to the apexes of lattices, and the other to the body centers of lattices.

Let J_{ev}'s be junction points of the former and J_{od}'s the latter. For either J_{ev}'s or J_{od}'s, two different spatial orientations per junction point can be allocated in the way of combination with four neighboring strands around a given junction point. The effects of these two arrangements, however, are essentially identical in view of contribution to the free energy of the system, so it doesn't matter which of them is chosen in going on disscussing. A J_{ev} in the central part of the system is usually selected as an origin of the coordinates. For convenience, letting the length of an edge of lattices be 2, we can describe readily the coordinates of every junction point as a set of three components having only values of integers. Characteristic combination modes of strands around the general junction points J_{ev}'s and J_{od}'s are plotted in Figure 4, where the spatial orientations of strands, in addition to the coordinates of junction points, are defined on the basis of a J_{ev}.

Letting c be a position vector representing, independently of J_{ev} or J_{od}, any junction point, three components of this and variation fields of components are given by, respectively,

$$\begin{aligned} &l=(i,\ j,\ k)\\ &i=-I,\ -I+1,\ \cdots,\ I-1,\ I\\ &j=-J,\ -J+1,\ \cdots,\ J-1,\ J\\ &k=-K,\ -K+1,\ \cdots,\ K-1,\ K \end{aligned} \tag{49}$$

where the I,J, and K are all positive integers. Note that the components of every J_{ev} all have values of even integers, and that those of every J_{od} have only values of odd integers. As plotted in Figure 4(b), spatial orientations of all the strands in the system are reduced to only four. For convenience, let σ_l or $\sigma_{i,j,k}$ ($\sigma = X, Y, Z$, and W) be the symbol denoting a strand. The four spatial orientations of strands in the system are defined by

$$\begin{aligned} X_{i,j,k}&=\text{strand from } J_{ev}(i,j,k) \text{ to } J_{od}(i-1,j+1,k+1)\\ Y_{i,j,k}&=\text{strand from } J_{ev}(i,j,k) \text{ to } J_{od}(i+1,j-1,k+1)\\ Z_{i,j,k}&=\text{strand from } J_{ev}(i,j,k) \text{ to } J_{od}(i+1,j+1,k-1)\\ W_{i,j,k}&=\text{strand from } J_{ev}(i,j,k) \text{ to } J_{od}(i-1,j-1,k-1) \end{aligned} \tag{50}$$

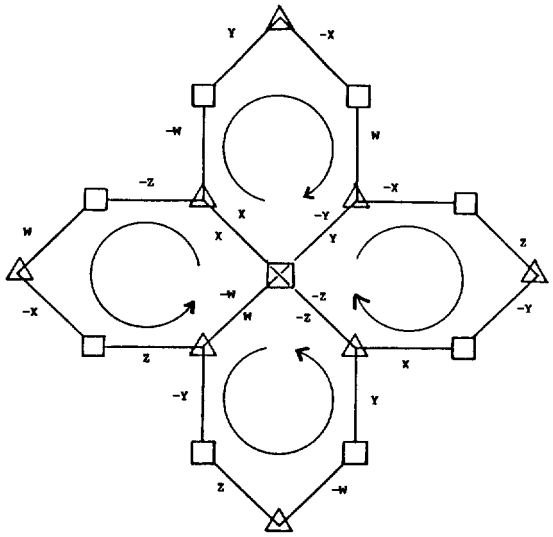

Figure 5. A diagram representing directions of rotation of loops and four hexagonal unit loops around a J_{ev}. Small squares represent the J_{ev}'s and small triangles the J_{od}'s.

where the picture for these orientations is shown in Figure 4(b). Though the number of loops formed around a J_{ev} is all 12, these are reduced to only four unit loops, that is, 12 loops can be represented by the linear combination of 4 unit loops. In similarity to the case of strands, let u_l or u_{ijk} ($u=\xi,\eta,\zeta$, and δ) be the symbol denoting a loop. The four unit loops, which are all hexagonal types consisting of 6 strands, around a $J_{ev}(i,j,k)$ are expressed by

$$\begin{aligned} \xi_{ijk}&=X_{ijk}-W_{i,j+2,k+2}+Y_{i,j+2,k+2}-X_{i+2,j,k+2}+W_{i+2,j,k+2}-Y_{ijk}\\ \eta_{ijk}&=Y_{ijk}-X_{i+2,j-2,k}+Z_{i+2,j-2,k}-Y_{i+2,j,k-2}+X_{i+2,j,k-2}-Z_{ijk}\\ \zeta_{ijk}&=W_{ijk}-Y_{i-2,j,k-2}+Z_{i-2,j,k-2}-W_{i,j+2,k-2}+Y_{i,j+2,k-2}-Z_{ijk}\\ \delta_{ijk}&=X_{ijk}-Z_{i-2,j,k+2}+W_{i-2,j,k+2}-X_{i-2,j-2,k}+Z_{i-2,j-2,k}-W_{ijk} \end{aligned} \tag{51}$$

where the minus symbols attached to terms of the right-hand sides denote the inverse of orientation of given strands. Thus, the orientation of rotation of unit loops also is described in Eq. 51. All the relationships for 4 unit loops stated up to now are shown apparently in Figure 5, where the symbols of cyclic arrows denote the orientation of rotation of loops, small squares represent J_{ev}'s, and small triangles are J_{od}'s.

The letters X, Y, Z, and W denoted along loops represent the orientation of strands, defined by Eq. 50. In describing junction points of lattices, it is usually convenient to discuss the physical properties of the system by separating J_{ev}'s and J_{od}'s respectively. Since the distinction of J_{od}'s and J_{ev}'s derives only from the description of the coordinates, the formation mode of 12 hexagonal loops around any junction point is exactly identical for either a J_{ev} or a J_{od}. After considering the system composed of only J_{ev}'s, we can also apply the information obtained above to the system of only J_{od}'s. Thus, first we consider the system composed of only J_{ev}'s. We can see readily that the structure of lattices in this system is that of the SCL's.

Let i be the coordinate system of junction points, including all J_{ev}'s and J_{od}'s, along the x- axis, then we have

$$\begin{aligned} &i=-I, I+1, \cdots, I-1, I\\ &I=2Q \end{aligned}$$

$$i' = -2Q, -2Q+2, \cdots, 2Q-2, 2Q \qquad (52)$$
$$q \equiv i'/2 = -Q, -Q+1, \cdots, Q-1, Q$$

where the letters I and Q denote positive integers, and in particular, I is a positive even integer. In similarity to the x-axis system, along the axes y and z the following relationships are given by

$$\begin{aligned} J &\equiv 2R \\ r &\equiv j'/2 \\ K &\equiv 2S \\ s &\equiv k'/2 \end{aligned} \qquad (53)$$

where J and r correspond to the y-axis, and K and s to the z-axis. Now expressing Eq. 51 as the newly reduced coordinate system (q,r,s), we obtain a series of equations given by

$$\begin{aligned} \xi_{qrs} &= X_{qrs} - W_{qr+1s+1} + Y_{qr+1s+1} - X_{q+1rs+1} + \\ &\quad W_{q+1rs+1} - Y_{qrs} \\ \eta_{qrs} &= Y_{qrs} - X_{q+1r-1s} + Z_{q+1r-1s} - Y_{q+1rs-1} \\ &\quad + X_{q+1rs-1} - Z_{qrs} \\ \zeta_{qrs} &= W_{qrs} - Y_{q-1rs-1} + Z_{q-1rs-1} - W_{qr+1s-1} \\ &\quad + Y_{qr+1s-1} - Z_{qrs} \\ \delta_{qrs} &= X_{qrs} - Z_{q-1rs+1} + W_{q-1r-1s} - X_{q-1r-1s} \\ &\quad + Z_{q-1r-1s} - W_{qrs}. \end{aligned} \qquad (54)$$

Eq. 54 is not arithmetic expressions, but symbolic ones. In Section 8, Eq. 54 will be transformed into arithmetic expressions. Also Eq. 54 is indispensable expressions leading to calculation of the projection matrix $\Gamma^{\#}$ of the BCL model. Since all the loops in the system are formed by exactly alternate linkings of J_{od}'s and J_{ev}'s, unit loops around any J_{od} take the same linking form of strands as that of J_{ev}'s given in Eq. 54.

Projection Matrix $\Gamma^{\#}$

It is assumed that the network composed of lattices is cyclic in the direction of the axes x,y, and z, respectively. For junction points, strands, and loops, respectively, it is assumed that

$$\begin{aligned} &J_{Q+1rs} = J_{-Qrs}, \quad J_{qR+1s} = J_{q-Rs}, \quad J_{qrS+1} = J_{qr-S} \\ &\sigma_{Q+1rs} = \sigma_{-Qrs}, \quad \sigma_{qR+1s} = \sigma_{q-Rs}, \quad \sigma_{qrS+1} = \sigma_{qr-S} \\ &U_{Q+1rs} = U_{-Qrs}, \quad U_{qR+1s} = U_{q-Rs}, \quad U_{qrS+1} = U_{qr-S} \end{aligned} \qquad (55)$$

where J's denote junction points, and σ's and U's represent strands and loops, respectively. All the coordinate systems used in this section are equal to those of Section 7. Let σ_{qrs} and U_{qrs} be expressed as the form of triple products, that is,

$$\begin{aligned} \sigma_{qrs} &\equiv \sigma_q \sigma_r \sigma_s \\ U_{qrs} &= U_q U_r U_s \end{aligned} \qquad (56)$$

where though single terms of the right-hand sides have no physical meanings, triple product terms, each of which is composed of three single terms, have the same physical meanings as terms given in the left-hand sides. As stated previously, σ's denote strands, and U's loops. Letting σ_L and U_L be all $(2L+1)$-dimensional row vectors, row vectors of strands and loops are expressed by

$$\begin{aligned} X_Q &= (X_Q X_{Q-1} \cdots X_{-Q+1} X_{-Q}) \\ X_R &= (X_R X_{R-1} \cdots X_{-R+1} X_{-R}) \\ &\cdots\cdots \\ \delta_R &= (\delta_R \delta_{R-1} \cdots \delta_{-R+1} \delta_{-R}) \\ \delta_S &= (\delta_S \delta_{S-1} \cdots \delta_{-S+1} \delta_{-S}). \end{aligned} \qquad (57)$$

From Eqs. 56 and 57, σ and U take the form of row vectors given by

$$\begin{aligned} \sigma &= (X \; Y \; Z \; W) \\ U &= (\xi \; \eta \; \zeta \; \delta) \end{aligned} \qquad (58)$$

where the $X, Y, Z, \cdots, \eta, \xi$, and δ are expressed by

$$\begin{aligned} X &= X_Q \otimes X_R \otimes X_S, \quad & Y &= Y_Q \otimes Y_R \otimes Y_S \\ Z &= Z_Q \otimes Z_R \otimes Z_S, \quad & W &= W_Q \otimes W_R \otimes W_S \\ \xi &= \xi_Q \otimes \xi_R \otimes \xi_S, \quad & \eta &= \eta_Q \otimes \eta_R \otimes \eta_S \\ \zeta &= \zeta_Q \otimes \zeta_R \otimes \zeta_S, \quad & \delta &= \delta_Q \otimes \delta_R \otimes \delta_S \end{aligned} \qquad (59)$$

the symbol $\otimes$ being a direct product between matrices. Let U_L be a $(2L+1)$-dimensional unit matrix given by

$$U_L = \begin{pmatrix} 1 & & & & & \\ & 1 & & & & \\ & & 1 & & & \\ & & \cdots & & & \\ & & & \cdots & 1 & \\ & & & & & 1 \end{pmatrix}$$

and let D_L be a $(2L+1)$-dimensional matrix defined by

$$D_L = \begin{pmatrix} 1 & & & & & & -1 \\ -1 & 1 & & & & & \\ & -1 & 1 & & & & \\ & & -1 & 1 & & & \\ & & & \cdots & & & \\ & & & & \cdots & & \\ & & & & & -1 & 1 \\ & & & & & & -1 \; 1 \end{pmatrix}$$

where all the blank parts in square brackets have the values of zeros, and such a usage will keep being used in expression of all the matrices appearing hereafter. Let a, b, and c be matrices given by

$$\begin{aligned} a &\equiv U_Q \otimes D_R \otimes D_S \\ b &\equiv D_Q \otimes U_R \otimes D_S \\ c &\equiv D_Q \otimes D_R \otimes U_S \end{aligned} \qquad (62)$$

where a,b, and c are all $[(2Q+1)(2R+1)(2S+1) \times (2Q+1)(2R+1)(2S+1)]$-dimensional matrices.

By use of Eqs. 60 to 62, Eq. 54 can be transformed from symbolic expressions into arithmetic ones. From the consideration of the loop ξ_{qrs} formed at a $J_{ev}(q,r,s)$, the $[(2Q+1)(2R+1)(2S+1)]$-dimensional row vector, which is the set of all the unit loops having the same modes as ξ_{qrs} in the system, in Eq. 59 can be expressed by the linear combination of the X, Y, Z, and W as follows:

$$\begin{aligned} \xi_{qrs} &= X_{qrs} - X_{q+1rs+1} + Y_{qr+1s+1} - Y_{qrs} \\ &\quad + W_{q+1rs+1} - W_{qr+1s+1} \\ &= X_q X_r X_s - X_{q+1} X_r X_{s+1} + Y_q Y_{r+1} Y_{s+1} - \\ &\quad Y_q Y_r Y_s + W_{q+1} W_r W_{s+1} - W_q W_{r+1} W_{s+1} \end{aligned} \qquad (63)$$

$$\begin{aligned} \xi = &- (X_Q D_Q) \otimes (X_R U_R) \otimes (X_S D_S) \\ &+ (Y_Q U_Q) \otimes (Y_R D_R) \otimes (Y_S D_S) \end{aligned}$$

$$+(W_Q D_Q)\otimes(W_R(-D_R))\otimes(W_S U_S)$$
$$=-X(D_Q\otimes U_R\otimes D_S)+Y(U_Q\otimes D_R\otimes D_S)$$
$$+W(D_Q\otimes(-D_R)\otimes U_S). \tag{64}$$

Substitution of Eq. 62 into Eq. 64 leads to

$$\xi=-Xb+Ya-Wc. \tag{65}$$

Similarly to Eq. 65, the following equations for η,ζ, and δ are obtained by

$$\begin{aligned}\eta&=-Xa-Yb-Zc\\ \zeta&=Yc-Zb-Wa\\ \delta&=Xc-Za-Wb.\end{aligned} \tag{66}$$

Rearrangement of Eqs. 65 and 66 leads to

$$(\xi\eta\zeta\delta)=(XYZW)\begin{pmatrix}-b&-a&0&c\\ a&-b&c&0\\ 0&-c&-b&-a\\ -c&0&-a&-b\end{pmatrix} \tag{67}$$

or

$$U=\sigma B \tag{68}$$

where B is defined by

$$B\equiv\begin{pmatrix}-b&-a&0&c\\ a&-b&c&0\\ 0&-c&-b&-a\\ -c&0&-a&-b\end{pmatrix}. \tag{69}$$

From Eq. 67 or 68, we see that the matrix B, which has a $[4(2Q+1)(2R+1)(2S+1)\times 4(2Q+1)(2R+1)(2S+1)]$ dimension, is a transformation matrix transforming loops into a linear combination of strands.

We define Σ and E to be

$$\begin{aligned}\Sigma&\equiv\sigma\otimes\sigma\\ E&\equiv U\otimes U.\end{aligned} \tag{70}$$

From Eq. 68 we obtain

$$E=\Sigma C \tag{71}$$

where C is defined by

$$C\equiv B\otimes B. \tag{72}$$

For a quick comparison with Eq. 70, it is advisable to transcribe Eq. 6 as follows:

$$T_0=\theta C,\quad T_1=\theta\Gamma. \tag{6}$$

Since E included all possible products of the type U_iU_i', and Σ, all possible products of the type $\sigma_i\sigma_{i'}$, the E and Σ are identified, respectively, to the T_0 and θ, and then Eq. 71 is reduced to the first equation of Eq. 6. Also it is apparent that C of Eq. 72 is equal to that of the first expression in Eq. 6.

Using the first equation of Eq. 11, we should find $C^{\#}$. From the character of matrices[17],

$$C^{\#}=B^{\#}\otimes B^{\#}. \tag{73}$$

Let M_L be an orthogonal matrix whose elements are defined by

$$[q_L]_{ll'}=\begin{cases}\sqrt{1/2L+1}\\ \sqrt{2/2L+1}\cos(2\pi ll'/2L+1)\\ \sqrt{2/2L+1}\sin(2\pi ll'/2L+1)\end{cases}$$

$$\begin{matrix}\text{for } l'=0\\ \text{for } l'=1,\cdots,L\\ \text{for } l'=-1,\cdots,-L.\end{matrix} \tag{74}$$

And let Δ_L be a diagonal matrix given by

$$\Delta_L\equiv\begin{pmatrix}d_L&&&\\ &d_{L-1}&&\\ &&\cdots&\\ &&&d_{-L}\end{pmatrix} \tag{75}$$

where the l'th diagonal element is

$$d_{l'}=2\sin^2(\pi l'/2L+1). \tag{76}$$

D_L is rearranged into

$$D_L=M_L^t\,\Delta_L M_L. \tag{77}$$

Substitution of Eq. 77 into Eq. 62 leads to

$$B=P^t FP \tag{78}$$

where the F and P are given by

$$F\equiv\begin{pmatrix}-\beta&-\alpha&0&\gamma\\ \alpha&-\beta&\gamma&0\\ 0&-\gamma&-\beta&-\alpha\\ -\gamma&0&-\alpha&-\beta\end{pmatrix},\quad P=\begin{pmatrix}M&&&\\ &M&&\\ &&M&\\ &&&M\end{pmatrix} \tag{79}$$

where elements of the right-hand sides take the form of

$$\begin{aligned}\alpha&=U_Q\otimes\Delta_R\otimes\Delta_S\\ \beta&=\Delta_Q\otimes U_R\otimes\Delta_S\\ \gamma&=\Delta_Q\otimes\Delta_R\otimes U_S\\ M&=M_Q\otimes M_R\otimes M_S.\end{aligned} \tag{80}$$

In above equations, α,β, and γ are all diagonal matrices because all these are given by direct products of diagonal matrices. For example, expressions of α,β, and γ are expressed, respectively, by

$$\begin{aligned}\alpha_{R,S}&=\begin{pmatrix}\alpha_{1(2R+1)(2S+1)}\\ \alpha_{1(2R+1)(2S+1)-1}\\ \cdots\end{pmatrix}\\ \beta_{Q,S}&=\begin{pmatrix}\beta_{1(2Q+1)(2S+1)}\\ \beta_{1(2Q+1)(2S+1)-1}\\ \cdots\end{pmatrix}\\ \gamma_{Q,R}&=\begin{pmatrix}\gamma_{1(2Q+1)(2R+1)}\\ \gamma_{1(2Q+1)(2R+1)-1}\\ \cdots\end{pmatrix}\end{aligned} \tag{81}$$

where the detailed forms of elements in square brackets are given by

$$\begin{aligned}\alpha_{r,s}&=4\sin^2(\pi r/2R+1)\cdot\sin^2(\pi s/2S+1)\\ \beta_{q,s}&=4\sin^2(\pi q/2Q+1)\cdot\sin^2(\pi s/2S+1)\\ \gamma_{q,r}&=4\sin^2(\pi q/2Q+1)\cdot\sin^2(\pi r/2R+1).\end{aligned} \tag{82}$$

Since P is the orthogonal matrix, we obtain

$$B^{\#}=(P^tFP)^{\#}=P^{\#}F^{\#}P \tag{83}$$

where $F^{\#}$ is the projection matrix of F. Since F is a 4×4 super matrix whose elements are all diagonal matrices of the same dimension, it can be transformed into the following

Table 1. Values of $B^{\#}$ (σ_{000}, $\sigma'_{q,r,s}$) for $Q=R=S=16$

(q,r,s)	(σ,σ') (X,X)	(X,Y)	(X,Z)	(X,W)	(Y,Z)	(Y,W)	(Z,W)
(0,0,0)	-0.2304	-0.2304	0.1625	0.1463	-0.2204	0.2481	0.6774
(0,0,1)	0.4310	0.1325	-0.2742	0.4310	0.0012	-0.0042	0.4310
(0,0,2)	0.0438	0.0382	-0.0273	-0.0547	0.0224	0.0394	-0.0273
(0,1,14)	0.0824	-0.0631	0.0431	-0.0228	0.0119	-0.2418	0.0012
(0,1,15)	-0.0421	0.0339	0.0229	-0.0421	-0.0116	0.0175	0.0033
(0,1,16)	-0.0327	-0.0533	0.0420	0.0668	0.0241	0.0082	0.0082
(1,0,0)	0.2104	0.0448	0.2174	0.0271	-0.0172	0.0004	-0.0172
(1,0,1)	0.0661	-0.0272	-0.0182	0.0664	0.0084	-0.0064	0.0213
(1,0,2)	0.0588	0.0171	-0.0174	0.0448	0.0669	-0.0081	-0.0174
(2,16,0)	0.0072	0.0041	0.0082	-0.0412	0.0014	0.0041	0.0017
(2,16,1)	-0.0332	-0.0913	0.0172	-0.0027	0.0008	0.0172	0.0062
(2,16,2)	0.0994	0.0881	0.0851	0.0121	-0.0051	-0.0816	-0.0001
(8,8,8)	0.0082	0.0043	-0.0058	0.0013	0.0043	-0.0019	0.0094
(16,15,14)	0.0024	0.0012	0.0011	-0.0011	0.0010	0.0011	0.0004
(16,15,15)	0.0836	0.0811	-0.0810	-0.0014	0.0172	-0.0810	0.0043
(16,15,16)	0.0996	-0.0732	0.0120	0.0144	-0.0732	0.0182	0.1011
(16,16,14)	-0.1014	0.0999	-0.0082	0.1014	-0.0795	0.0682	0.0541
(16,16,15)	-0.0335	0.0114	0.0023	0.0249	0.0248	0.0413	-0.0311
(16,16,16)	0.0227	0.1624	0.1463	-0.1732	0.2432	0.2304	-0.0129

block matrix by changing orders of row and column vectors properly:

$$F=\begin{pmatrix} f_\lambda & & & \\ & f_{\lambda'} & & \\ & & f_{\lambda''} & \\ & & & \cdots \end{pmatrix} \tag{84}$$

$$f_\lambda=\begin{pmatrix} -\beta_{q,s}-\alpha_{r,s} & 0 & \gamma_{q,r} \\ \alpha_{r,s}-\beta_{q,s} & \gamma_{q,r} & 0 \\ 0 & -\gamma_{q,r}-\beta_{q,s}-\alpha_{r,s} & \\ -\gamma_{q,r} & 0 & -\alpha_{r,s}-\beta_{q,s} \end{pmatrix} \tag{85}$$

where $\lambda=(q,r,s)$.

Thus,

$$F^{\#}=\begin{pmatrix} f_\lambda{}^{\#} & & & \\ & f_{\lambda'}{}^{\#} & & \\ & & f_{\lambda''}{}^{\#} & \\ & & & \cdots \end{pmatrix} \tag{86}$$

where $f^{\#}_{\lambda}$, $f^{\#}_{\lambda'}$, $\cdots$ are projection matrices of f_λ, $f_{\lambda'}$, $\cdots$ given by Eq. 86. After the matrices $f^{\#}_{\lambda}$, $f^{\#}_{\lambda'}$, $\cdots$ are calculated numerically for the large value of Q,R, and S, they can be transformed into $B^{\#}$ with use of Eq. 83.

As exposed in Eq. 69, since $B^{\#}$ has highly symmetric structure, it is sufficient to find elements of $B^{\#}$ only for the strand pair σ_{000} and σ'_{qrs} ($\sigma,\sigma' = X,Y,Z$, and W).

A number of elements of $B^{\#}$ for $Q=R=S=16$ are given in Table 1. In Table 1, since the strand pairs (X,X),(Y,Y), (Z,Z), and (W,W) all have the same values, they can be represented only as the (X,X). On the other hand, (X,Y) has the same value as (Y,X); (X,Z) as (Z,X); (X,W) as (W,X); $\cdots$; and (Z,W) as (W,Z). As a result, totally 7 of independent pairs (σ,σ')'s for any junction point are obtained.

To obtain $\Gamma^{\#}$ with the aid of the first equation of Eq. 11, we have only to find $C^{\#}$. Any element of $C^{\#}$ is given by direct products of two of $B^{\#}$s, Letting $\Gamma^{\#}[(\sigma_{qrs},\sigma'_{q'r's'})(\sigma''_{q''r''s''},\sigma'''_{q'''r'''s'''})]$ be an element of the matrix $\Gamma^{\#}$ for the pairs $(\sigma_{qrs},\sigma'_{q'r's'})$ and $(\sigma''_{q''r''s''},\sigma'''_{q'''r'''s'''})$, we have

$$\begin{aligned}&\Gamma^{\#}[(\sigma_{qrs},\sigma'_{q'r's'})(\sigma''_{q''r''s''},\sigma'''_{q'''r'''s'''})] \\ &=B^{\#}(\sigma_{000},\sigma'_{(q'-q)(r'-r)(s'-s)}) \cdot \\ &\quad B^{\#}(\sigma''_{000},\sigma'''_{(q'''-q'')(r'''-r'')(s'''-s'')})\end{aligned} \tag{87}$$

with which all the other elements of $\Gamma^{\#}$ are obtained.

Having calculated the projection matrix $\Gamma^{\#}$ of the BCL model, we can calculate F_2 by using Eqs. 24 and 87. Thus we can compute completely the total free energy of the network through the process discussed up to now.

Application to the Sample PDMS

The process of formation of the sample PDMS(poly(dimethyl siloxane)) is as follows:

$$n(CH_3)_2SiCl_2+nH_2O\longrightarrow-\left[-O-\overset{CH_3}{\underset{CH_3}{Si}}-\right]_n-+2n\ HCl \tag{88}$$

PDMS ($M_w=74.0$, $b=5.7$ Å)

where M_w and b are the molecular weight and the length of a segment of the PDMS, respectively. Recall that as referred to earlier, a strand denotes a polymer chain which is fixed at any two of junction points. If we let ν be the degree of polymerization, which corresponds to the number of segments in a strand, such polymers as polyisoprene, polystyrene, and PDMS have the values of about 30 to 300.[17] It is assumed that the whole system of the PDMS is composed of the BCL's. A cell consists of 8 subcells, and the structure of a subcell is plotted in Figure 6. Thus a cell has 128 junction

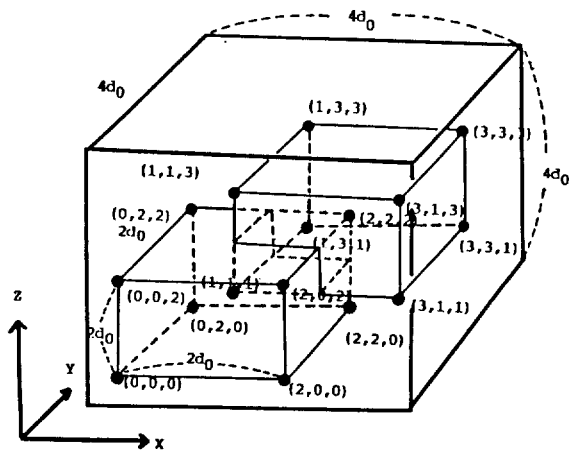

Figure 6. A diagram representing the structure of a subcell and the coordinates of its junction points. The size of a subcell, which is composed of 16 junction points and 32 strands, is $(4d_0)(4d_0)(4d_0)$. A cell is composed of 8 subcells. Thus a cell has 128 junction points and 256 strands.

points and 256 strands.

Now consider the relationship between cells and the whole lattice system. Letting l,m, and p be the sets of the coordinates of integers along the axes x,y, and z, respectively, we have

$$\begin{aligned} l &= -8L,\ -8L+1,\ \cdots,\ -1,\ 0,\ 1,\ \cdots,\ 8L-2,\ 8L-1 \\ m &= -8M,\ -8M+1,\ \cdots,\ -1,\ 0,\ 1,\ \cdots,\ 8M-2,\ 8M-1 \\ p &= -8P,\ -8P+1,\ \cdots,\ -1,\ 0,\ 1,\ \cdots,\ 8P-2,\ 8P-1 \end{aligned} \tag{89}$$

where the L,M, and P are all positive integers. if we let C_N be the number of cells, and N_{jev} that of junction points belong to apexes of lattices, a series of the following expressions are obtained by

$$\begin{aligned} C_N &= (2L)\ (2M)\ (2P) = 8\ LMP \\ N_0 &= 128\,C_N = 1024\ LMP \\ S_N &= 2N_0 = 2048\ LMP \\ N_{jev} &= N_{jod} = N_0/2 = 512\ LMP \end{aligned} \tag{90}$$

where N_0 is the sum of N_{jev} and N_{jod} and S_N is the number of strands. In an actual calculation, we take $L = M = P = 4$, and then l,m, and p have the variation fields of integers as

$$\begin{aligned} l &= -32,\ -31,\ \cdots,\ 30,\ 31 \\ m &= -32,\ -31,\ \cdots,\ 30,\ 31 \\ p &= -32,\ -31,\ \cdots,\ 30,\ 31 \end{aligned} \tag{91}$$

where these variation fields are almost equal to those of Iwata[17] for the SCL model. Alternatively, physical properties of the whole lattice system can be fully described only by the lattice size of such a extent. Though the size of the lattice system is increased more, all the calculated values of the increased system are retained, if any, almost unchangeably. In the region of Eq. 91, C_N has the value of 512, N_0 that of 65,536, and S_N that of 131,072.

The value of ν', which is the term necessary in the calculation of the $g_p(r)$ and $h_p(r)$ given by Eq. 16, is fixed at 10, which equals that of Iwata[17] for the SCL model. Since the more increased the value of ν' is the more delayed the time required in the calculation of the computer is at the fourth power of ν', it seems that the value of 10 for ν' is the upper limit of the computer used, and that the value gives enough accuracy in the calculation of the free energy of the network.

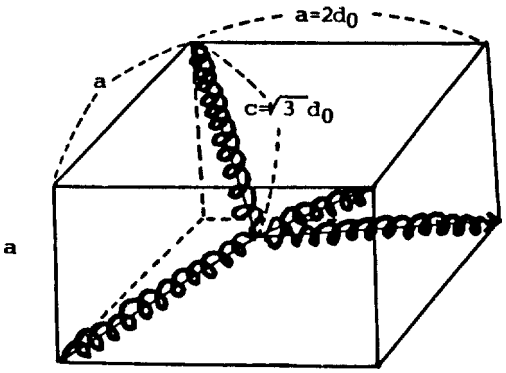

Figure 7. The length relationship of strands, which is in the standard configuration, of the pressed spring structures combined with four junction points in a lattice of the BCL system.

Results and Discussion

The whole three dimensional form of the BCL model is shown in Figure 3. Only one of their lattices is plotted in Figure 7. At this stage it is necessary to introduce the concept of the standard configuration. As shown in Figure 7, the standard configuration denotes the form of arrangement in which all the strands are arranged linearly with all the strands pressed tightly in the form of springs. In the calculation of projection matrices of Section 8, the standard configuration of lattices has been taken as the reference state of the system. Now we introduce a parameter δ related to the standard configuration.

As shown in Figure 7, letting $2d_0$ be the length of an edge of the lattice, the length of a strand must be $\sqrt{3}\,d_0$ in the standard configuration. Since the value of $\sqrt{3}\,d_0$ is the linear length of a strand in the state pressed tightly in the form of springs, if the pressed state of a strand is released, that is, if a strand extends in random state, the actual length of a strand will become longer.

In the state of the phantom network, the distance from the center to an apex in a lattice corresponds to the root mean squared end-to-end length, that is, $\sqrt{\nu}\,b$, of a strand. Recall that the definition of b and ν has already been stated in Section 9. Now the definition of δ is given by the ratio of the end-to-end distance of a strand in the standard configuration versus that of a strand in the phantom network, that is,

$$\delta = \sqrt{3}\,d_0/(\sqrt{\nu}\,b). \tag{92}$$

The density of strands of an unit lattice C_e and the reduced distance δ are expressed by

$$C_e = 4\,(M_w/N_A)\,\nu/(2d_0)^3 \tag{93}$$

$$\begin{aligned} \delta &= (\sqrt{3}/2)\,(4M_w/N_A)^{1/3} \cdot C_e^{-1/3} \cdot \nu^{-1/6} \cdot b^{-1} \\ &= 6.834\times10^{-8} C_e^{-1/3} \cdot \nu^{-1/6} \cdot b^{-1} \end{aligned} \tag{94}$$

where N_A is the Avogadro's number. The coefficient 6.834×10^{-8} of Eq. 94 is obtained by allocating values of 74.0 to M_w. In Eq. 94, C_e is represented as the unit of g/cm^3, and b as that of cm.

Typical elastic polymers, such as polyisoprene, polys-

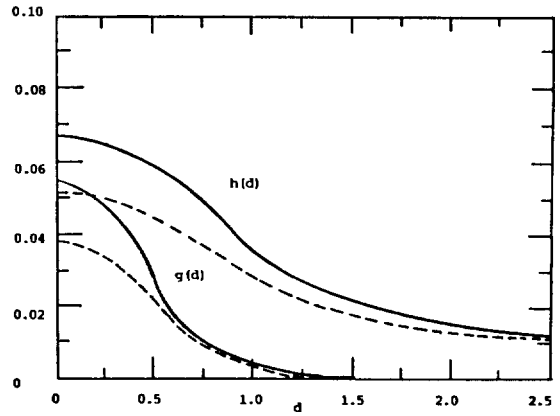

Figure 8. The $g_p(d)$ and $h_p(d)$ as functions of d, which is a distance between the centers of the strands, for the BCL model. Solid lines represent curves obtained when the root mean squared end-to-end distance of a strand is $0.5\sqrt{\nu}\,b$, and dashed lines denote curves obtained when that of a strand is $\sqrt{\nu}\,b$, where ν is the degree of polymerization and b the length of a segment in the PDMS.

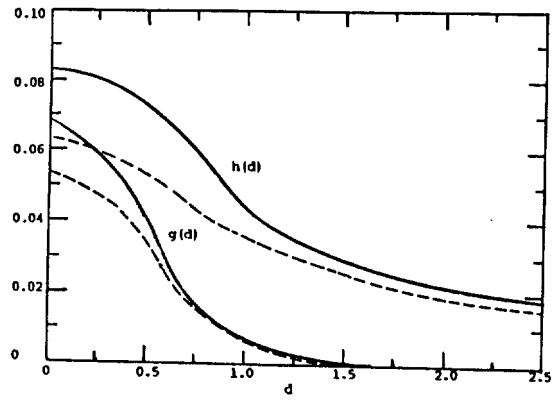

Figure 9. The $g_p(d)$ and $h_p(d)$ as functions of d for the SCL model. The notations are the same as those of Figure 8.

tyrene, PDMS, and etc. whose ν values are given as 30 to 300, have the δ values of 0.5 to 0.8. The functions $g_p(r)$ and $h_p(r)$ given in Eq. 16 can be easily transformed into the functions $g_p(d)$ and $h_p(d)$, d being given by Eq. 35. The functions $g_p(d)$ and $h_p(d)$ are plotted according to the BCL model in Figure 8, and according to the SCL model in Figure 9. In Figures 8 and 9, solid lines represent curves obtained when the root mean squared end-to-end distance of a strand is $0.5\sqrt{\nu}b$, and dashed lines denote curves obtained when that of a strand is $\sqrt{\nu}b$. In Figures 8 and 9, the value of $h_p(d)$ is greater than that of $g_p(d)$ because the double contact probability is greater than the single contact one due to the character resulting from the relatively long length of a strand. As the value of d is increased, the values of $g_p(d)$ and $h_p(d)$ become smaller, for the increase of the reduced distance d decreases the contact probability between two strands.

Also according to the relative ratio of occupation of junction points per strand, the height of curves in the BCL model is higher than that of curves in the SCL model. From the character of distribution functions in the phantom network, we can see that the general shape of curves is similar in two models. For the simple deformation considered here, we have

$$\lambda_x = \lambda_y = \lambda^{-1/2} \tag{95}$$

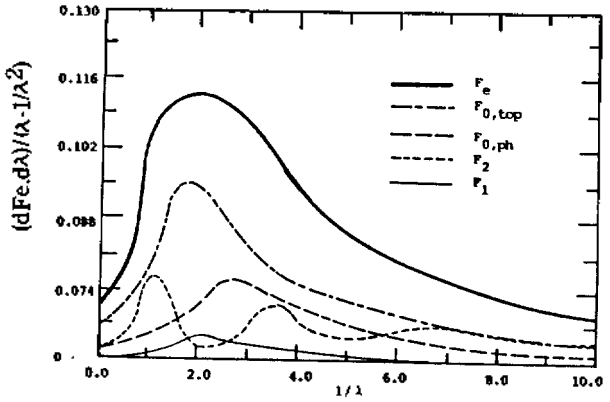

Figure 10. The curves representing the total free energy of the network and the four energy terms of which the total free energy is composed for the BCL model.

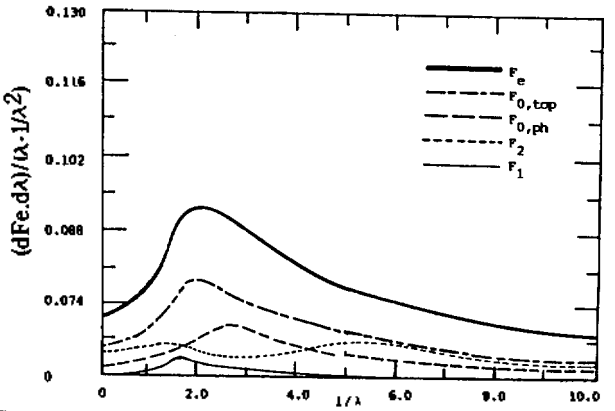

Figure 11. The curves representing the total free energy of the network and the four energy terms of which the total free energy is composed for the SCL model.

$$\lambda_z = \lambda .$$

Similarly to the SCL model, in the calculation of the $<V^*>$, $<V^*V^*>$, and $<W^*>$, the contribution of strand pairs included in the right-hand sides of Eqs. 39 to 41 satisfies that

$$d = (d_x, d_y, d_z) = \frac{|r_a + r_a' - r_b - r_b'|}{2\sqrt{\nu}\,b} \tag{35}$$

$$d_x^2 + d_y^2 + d_z^2/Z \geqq \begin{cases} 5 & \text{for } \lambda \geqq 1 \\ 4 & \text{for } \lambda < 1 \end{cases} \tag{96}$$

$$Z = \begin{cases} 1 & \text{for } \lambda \geqq 1 \\ 1.5 & \text{for } \lambda < 1 \end{cases} \tag{97}$$

$$g_{ab}^0 \geqq \begin{cases} 10^{-7} & \text{for } \lambda \geqq 1 \\ 10^{-9} & \text{for } \lambda < 1 \end{cases} \tag{98}$$

where the weighted value Z in the z-axis is given to consider this unbalanced effect of the strain acting only along the x-axis. Since the value of g_{ab} is closely influenced by that of λ before and behind 1, the weighted value Z and g_{ab}^0 are changed at $\lambda = 1$.

In Figures 10 and 11, F and four components of that are plotted according to the BCL model and the SCL model, respectively. The contribution of F_2 to F is greater in the BCL model of Figure 10 than in the SCL model of Figure 11. It seems that such a phenomenon results from the fact that the

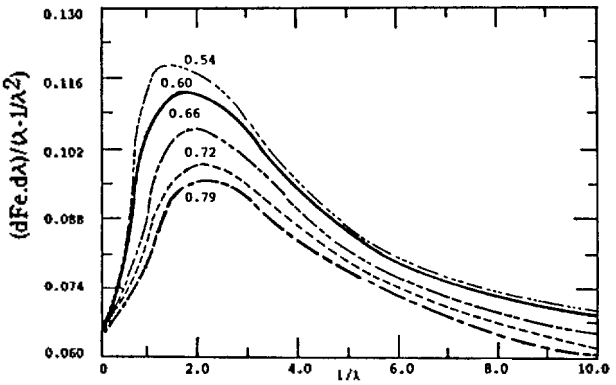

Figure 12. The curve representing the variation modes according to the parameter δ for the BCL model.

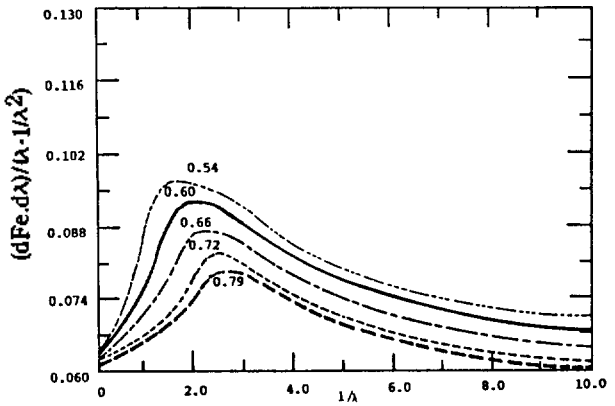

Figure 13. The curves representing the variation modes according to the parameter δ for the SCL model.

contribution of junction points per strand is greater in the BCL model than in the SCL model. Figures 10 and 11 show that the main contribution to F is $F_{0,top}$.

The changing modes of free energy curves along the values of δ are shown in Figures 12 and 13, where the more decreased the degree of polymerization is, the more increased the value of δ is because that as the values of ν are increased, the contact probabilities of strands are increased, and then contribution to F also becomes more increased. As the values of σ are decreased, the peaks of the energy curves are moved to the left of the x-axis. It seems that the reason why such a phenomenon arises is due to the fact that the increase of ν lets the interaction between strands be influenced sensitively by the values of λ after and behind 1.

With the experimental results[20] represented by small circles, the topological calculated curves, in the BCL model and in the SCL model, and the statistically calculated curve of Flory[19,23-25] are plotted in Figure 14. In the statistical entanglement model, which has two parameters[19] $k = 10$ and $\xi = 0.05$, of Flory, a departure from the Mooney-Rivlin form for the stress versus strain curve has been explained as the contribution of constraint energies restricting movement of junction points. On the other hand, in the topological BCL model, which has only one parameter $\delta = 0.62$, of the authors, a departure from the Mooney-Rivlin form for the stress versus strain curve can be explained as the topological interaction between strands in the network. Thus it can be stated that the topological interaction in the BCL model corresponds to the constraint energy in the statistical entanglement model.

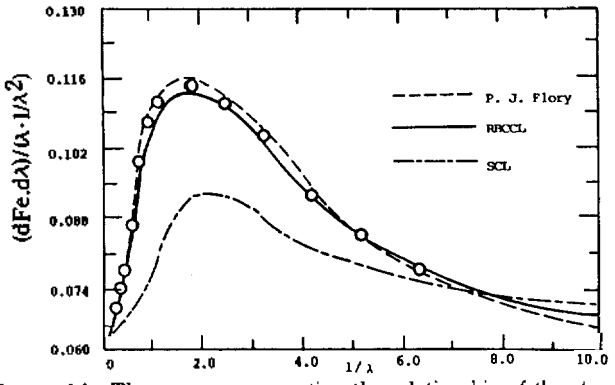

Figure 14. The curves representing the relationship of the stress versus strain on the PDMS sample. Here the curve of the BCL model is compared with that of the statistical entanglement model of P. J. Flory, with that of the topological SCL model of K. Iwata, and with the experimental data depicted by small circles.

For the statistical model though the general explanation on the experimental data has been successful, since topological effects of junction points and strands in the system have not been considered, and since individual contributions of junction points and strands to the total energy have not been stated in detail, a theoretical reformation for this model may be indispensable. On the other hand, for the topological model, since the results calculated from this topological model also have been in good agreement with the experimental data for the PDMS, and since the deficiency in the model of Flory has been completed almost entirely, it is regarded, in view of the theoretical background, that the topological BCL model is better than the statistical entanglement model.

From the results of two models above and in the departure of the topological SCL model from the experimental data, we can assert that the PDMS used as a sample[20] has the tetrahedral structure of strands around junction points.

Finally, the authors would like to point out that significance for the application of the topological BCL model to the PDMS can be found in the fact that a great number of papers[19,21-25] have been published by regarding the experimental data of the PDMS[20] as the standard values of polymer experiments.

Acknowledgement. The authors thank the Daewoo Foundation for financial support during this work.

References

1. H. M. James, *J. Chem. Phys.* **15,** 651 (1936).
2. W. Kuhn, *Kolloid, Z.* **76,** 258 (1936); *Angev. Chem.* **51,** 640 (1938).
3. T. F. Wall, *J. Chem. Phys.* **10,** 132 (1942); **11,** 527 (1943).
4. H. M. James and E. Guth, *J. Chem. Phys.* **11,** 455 (1943); **15,** 669 (1947); *J. Polym. Sci.* **4,** 153 (1949).
5. L. R. G. Treloar, *Trans. Faraday Soc.* **39,** 36 (1943).
6. P. J. Flory and J. Rehner, Jr., *J. Chem. Phys.* **11,** 521 (1943).
7. S. F. Edwards and K. F. Freed, *J. Phys. C.* **3,** 760 (1970).
8. K. F. Freed, *J. Chem. Phys.* **55,** 5588 (1971).
9. W. W. Graessley, *Macromolecules,* **8,** 865 (1975).
10. G. Ronca and G. Allegera, *J. Chem. Phys.* **63,** 4990 (1975).

11. P. J. Flory, *Proc. R. Soc. London Ser. A* **351**, 351 (1976).
12. A. Ziabicki and J. Walasek, *Macromolecules*, **11**, 471 (1978).
13. R. T. Deam and S. F. Edwards, *Philos. Trans. R. Soc. London Ser. A* **280**, 317 (1976).
14. W. W. Graessley and D. S. Pearson, *J. Chem. Phys.* **66**, 3363 (1977).
15. N. R. Langley, *Macromolecules*, **1**, 348 (1968); N. R. Langley and K. E. Polmansteer, *J. Polym. Sci.* **12**, 1023 (1974).
16. K. Iwata, *J. Chem. Phys.* **73**, 562 (1980); **74**, 2039 (1981); **78**, 2778 (1983); **83**, 1969 (1985).
17. K. Iwata, *J. Chem. Phys.* **76**, 6363 (1982); *ibid*, 6375 (1982).
18. K. Iwata and M. Kurata, *J. Chem. Phys.*, **50**, 4008 (1969).
19. P. J. Flory and B. Erman, *Macromolecules*, **15**, 800 (1982); B. Erman and P. J. Flory, *ibid*, 806 (1982).
20. H. Pak and P. J. Flory, *J. Polym. Sci.*, **17**, 1845 (1979).
21. J. Kovac and C. C. Crabb, *Macromolecules*, **19**, 1744 (1986).
22. R. Ullman, *Macromolecules*, **19**, 1748 (1986).
23. P. J. Flory, *Polym. J.*, **17**, 1 (1985)
24. P. J. Flory, *J. Chem. Phys.*, **66**, 5720 (1977).
25. B. Erman and P. J. Flory, *J. Chem. Phys.*, **68**, 5363 (1978).
26. G. Strang, 'Linear Algebra and its Applications' (Academic Press, New York, 1976).

Isotope Selectivity in the CO_2 Laser Induced Decomposition of Trichloroethylene-H and Trichloroethylene-D

Sang Man Koo, Byung Soo Chun, and Kwang Yul Choo*

Department of Chemsitry, Seoul National University, Seoul 151-742. *Received October 17, 1988*

The infrared multiphoton decomposition of trichloroethylene-H(TCE-H) and trichloroethylene-D(TCE-D) was studied by using the high power CO_2 laser. The pressure dependence of TCE-H decomposition showed that the HCl elimination channel to form ClC ≡ CCl was the major step at high pressures, while the HC ≡ CCl formation step became important at low pressures.

$$Cl_2C = CHCl \xrightarrow{\text{high pressure}} ClC \equiv CCl + HCl$$

$$\xrightarrow{\text{low pressure}} HC \equiv CCl + 2Cl\cdot(Cl_2)$$

The IRMPD of TCE-H and TCE-D mixtures with 10P(20) laser line showed that optimum conditions of large isotope selectivity were the low system pressures and high laser powers. The experimentally observed dependence of the branching ratios on the pressure and laser fluence, and the isotope selectivity coefficients were quantitatively explained by using the modified energy grained master equations (EGME) model.

Introduction

In recent years the process of unimolecular dissociation by intense infrared radiation has been the subject of extensive studies. The initial impetus came from the very obvious practicality of *selective* multiphoton decomposition[1]. It is well understood that the IR selective nature can be effectively used in the isotope separation[2], and selective dissociation-elimination of unwanted impurities[3]. There have been many theoretical[4] and experimental papers dealing with selective multiphoton decomposition of various isotopes.

There are several approaches to LIS (Laser Isotope Separation), all of which rely on one common phenomena, the so-called "isotope shift", which theoretically makes possible the selective excitation. In practice, the separation is seldom achieved because of thermal collisions between molecules, because of the Doppler effect on the laser wavelengths, and because of anharmonicity, etc. When the absorption wavelengths of two isotopes are far apart, it is relatively easy to find and tune a laser to resonate at the absorption wavelength of one isotope, thus pumping energy into the selected isotope leaving no effect on unwanted isotope. For laser excitation to remain selective, there must be a minimization of collisional exchange of vibrational energy between the excited and unexcited isotope species.

During the last one and a half decade, many works on deuterium isotope separation have been reported. Typical molecules used for deuterium isotope separation were formaldehyde[5], freon 123[6], and fluoromethanes[7]. Other examples of laser isotope separation includes isotopes of boron (BCl_3), carbon (CF_3I, CF_3COCF_3) silicon(SiF_4), sulfur(SF_6), chlorine(CF_2Cl_2) selenium(SeF_6), molybdenium(MoF_6), Osmium(OsO_4 and Uranium(UF_6, $U(OCH_3)_6$) where the precursor molecules are indicated in the parentheses.

The IRMPD (Infrared Multiphoton Dissociation) of trichloroethylene-H (TCE-H) was previously investigated in molecular beam[8] and in static cell[9]. Lee and coworkers[8] observed that C-Cl bond fission, $C_2HCl_3 \rightarrow \cdot C_2HCl + Cl\cdot$, was a primary dissociation channel in their molecular beam-IRMPD system. In contrast to this Steinfeld and coworkers[9] reported that trichloroethylene underwent HCl elimination, $C_2HCl_3 \rightarrow HCl + C_2Cl_2$, as the mjaor reaction path at 10 torr TCE pressure in a static cell. Choo and coworkers[10] resolved the above apparent discrepancy by a detailed study on the